

NGC 7129 FIRS 2: an intermediate-mass counterpart of Class 0 objects

C. Eiroa¹, J. Palacios¹, and M.M. Casali²

¹ Departamento Física Teórica C-XI, Facultad de Ciencias, Universidad Autónoma de Madrid, Cantoblanco, E-28049 Madrid, Spain (carlos.javier@xiada.ft.uam.es)

² Royal Observatory, Blackford Hill, Edinburgh, EH9 3HJ, UK (M.Casali@roe.ac.uk)

Received 1 October 1997 / Accepted 20 March 1998

Abstract. We present JCMT (sub)millimetre observations of the young source NGC 7129 FIRS 2 and HIRAS maps of the whole NGC 7129 region. The total integrated luminosity of FIRS 2 is $\approx 430 L_{\odot}$. Its spectral energy distribution is described by a single-temperature grey body with $T = 35 K$ and $\beta = 0.9$. The total mass is found to be $\sim 6 M_{\odot}$. These and other properties indicate that FIRS 2 is an intermediate-mass counterpart of the low-mass Class 0 protostellar objects; in this sense, FIRS 2 is probably the youngest intermediate-mass object we know at present. The far-infrared emission of NGC 7129 is dominated by two sources: FIRS 1, which is located toward the HAeBe star LkH α 234, and FIRS 2. The cavity observed in the optical NGC 7129 reflection nebulosity and in radio emission lines is clearly observed in the HIRAS maps, particularly in the $25 \mu\text{m}$ band. The total estimated luminosity of the region is $\approx 4.5 \cdot 10^3 L_{\odot}$, consistent with the idea that the dust is heated by the cluster of HAeBe stars in NGC 7129.

Key words: stars: formation – ISM: individual objects: NGC 7129 FIRS 2 – infrared: stars

1. Introduction

In the first half of this decade, André et al. (1993) recognized a new class of cool, low-mass protostellar objects, which they called Class 0 sources and which are the youngest objects known, with ages of the order of $\leq 10^4$ years. Observationally, Class 0 objects (also often referred to as submillimetre protostars) are characterized by having strong submillimetre luminosity, no (or very weak) near-mid IR emission, and a spectral energy distribution (SED) which can be fitted by a single-temperature black body (André et al., 1993). The submillimetre luminosity is a relative measure of the total circumstellar mass, which is higher than the central stellar mass in the Class 0 sources (e.g. André 1997). Virtually all of them drive collimated molecular outflows (Bachiller 1996) and, in some cases, shock excited H₂ emission (e.g. Davis et al. 1994) or HH objects (Eiroa et al. 1994) have been detected. All the Class 0 sources known to date are low-luminosity objects and, consequently, low-mass

protostars (see the list compiled by Bachiller 1996). There is, however, no reason why more massive class 0 objects, the protostellar progenitors of Herbig AeBe (HAeBe) stars, should not also be detected. In fact, intermediate-mass stars have a pre-main sequence evolution with times spanning several 10^5 years (e.g. Palla & Stahler 1990, 1993).

NGC 7129 is a reflection nebula immersed in a very active and complex molecular cloud (see e.g. Hartigan & Lada 1985, Miranda et al. 1993, and references therein). The distance to the region has been estimated to be 1 kpc (Racine 1968), which is the value usually assumed for NGC 7129. Shevchenko & Yakubov (1989) have estimated a distance of 1250 ± 50 pc. In this paper, we will assume a value of 1 kpc for our calculations, since the small difference of both distance estimates does not qualitatively affect the main conclusions. The nebula is illuminated by several HAeBe stars, the most prominent being LkH α 234, which form part of a PMS stellar cluster. Bechis et al (1978) and Harvey et al. (1984) detected far-infrared extended emission and two point-like sources. One of these is associated with the star LkH α 234 and the second, called FIRS 2, lacks any optical or near-infrared counterpart. FIRS 2 coincides with a ¹³CO column density peak (Bechis et al. 1978), with a high-density NH₃ cloudlet (Güsten & Marcaide 1986), and is close to an H₂O maser (Rodríguez et al. 1980). In addition, a bipolar CO outflow is also associated with FIRS 2 (Edwards & Snell 1983).

In this work we present (sub)millimetre observations of FIRS 2 and IRAS maps of the whole NGC 7129 region. The main result of the analysis of these data is that FIRS 2 is an intermediate-luminosity object with properties similar to those of the low-mass Class 0 sources. This suggests that we have found a very young object, FIRS2, which is most likely to be an intermediate-mass counterpart of the Class 0 protostars.

2. Observations and results

2.1. (sub)millimetre observations

Submillimetre and millimetre continuum observations at 800, 1100, 1300 and 2000 μm of the source NGC 7129 FIRS 2 were carried out using the James Clerk Maxwell Telescope (JCMT) on Mauna Kea, Hawaii, on May, 1990. and the bolometer UKT14 (Duncan et al. 1990). Beam sizes were $19''$ FWHM

Table 1. IRAS and submillimetre fluxes of FIRS 2.

Wavelength (μm)	Flux (Jy)
25	5.4
60	91.2
100	195.2
800	5.82
1100	2.18
1300	1.49
2000	0.39

for 800, 1100 and 1300 μm , and $27''$ for 2000 μm . The signal from FIRS 2 was peaked up before commencing integration. Absolute calibration was achieved using Mars and Uranus assuming the brightness temperature of Griffin et al. (1986) and Orton et al. (1986), and filter passbands correct for 1 mm of water vapour. The likely uncertainty in the absolute flux of these calibrators is 5–10%. The consistency of the photometry was checked by observing other sources from the same observing run (Casali et al. 1993). Measured flux values are given in Table 1.

2.2. IRAS data

At SRON (Groningen, The Netherlands) we used the high-resolution image reconstruction algorithm (HIRAS) to produce IRAS 12, 25, 60 and 100 μm images of NGC 7129. HIRAS is a maximum entropy image restoration technique, which uses an interactive procedure giving a significant gain in spatial resolution and can approach the diffraction limit of the IRAS telescope, which ranges from $0'.4$ to $1'.7$. at 12 and 100 μm , respectively. A detailed description of the whole procedure is given by Bontekoe et al. (1994). In the final NGC 7129 HIRAS maps, positions of point-like sources differ randomly by $\approx 15''$ – $20''$, which is of the order of the default pixel-size, $15''$, used in the reconstructed HIRAS images. Therefore, the differences in positions are not meaningful within the spatial resolution. Fluxes have been estimated after removing the residual background, which remains left in the reconstructed images after applying the reconstruction procedure (see Bontekoe et al. 1994); in our case, it was practically zero at 12 μm and small values at other wavelengths.

Fig. 1 shows the HIRAS maps at 12, 25, 60 and 100 μm . Common to all wavelengths is the presence of a far-IR peak, FIRS 1, at the position of LkH α 234 and extended diffuse emission. A second prominent peak located southwards of the former is seen at 25, 60 and 100 μm . IRAS fluxes are given in Table 1. This peak coincides with the source FIRS 2 detected by Bechis et al. (1978) and Harvey et al. (1984). At 12 μm it seems to be a weak source close to this position; the angular distance from the 12 μm peak to any of the flux maxima at the other IRAS wavelengths is on average $\approx 40''$. This is twice as large as the offset in position found among the peaks of the IRAS bands for any other source in the maps. Thus, an association of the 12 μm source with FIRS 2 is doubtful. In addition, since the flux

from the 12 μm source is very low (≤ 0.2 Jy, background subtraction uncertain), the properties of FIRS 2 we deduce below and its nature are not significantly affected if such an association were real (for instance, the change of luminosity would be $< 3\%$). Therefore, we do not consider the 12 μm source in the following, although the emission of FIRS 2 at 12 μm should be clarified in the future. A pair of weak, secondary peaks are also seen in the shortest IRAS wavelengths. One of them, FIRS 3, coincides with the T Tauri star V 350Cep (see Miranda et al. 1994); the second one, FIRS 4, seems to be extended and is likely related to the reflection nebosity GM 1-53 (Magakian 1983), which is illuminated by the near-infrared source SVS 10, a B8-A0 star close to the main sequence (Strom et al. 1976, Magakian & Movsesian 1997). Table 2 gives 1950.0 coordinates, as measured at 25 μm , and fluxes of FIRS 3 and FIRS 4.

3. Discussion

3.1. FIRS 2

NGC 7129 FIRS 2 is neither visible in the optical nor in the near-infrared; in addition, it is point-like at far-infrared and (sub)millimetre wavelengths within the IRAS and JCMT spatial resolutions. Thus, it is most likely the youngest object detected in the region. The observed spectral energy distribution (SED) of FIRS 2 is shown in Fig. 2. The total integrated luminosity is $L_{\text{total}} \approx 430 L_{\odot}$, showing that FIRS 2 is a further intermediate-mass young stellar object in the region, although less massive than LkH α 234. The SED can be fitted assuming a grey-body of the form $S_{\nu} = B_{\nu,T}(1 - e^{-\tau_{\nu}})$, where $\tau_{\nu} = (\nu/\nu_c)^{\beta}$ and $B_{\nu,T}$ is the Planck function. The best χ^2 -fit ($\chi^2 = 0.073$) is achieved for $T = 35\text{K}$ and $\beta = 0.9$. There is a small excess at 25 μm which indicates that hotter dust is also present. The large fluxes emitted by FIRS 2 at smm and mm wavelengths in comparison to the total luminosity are remarkable. For instance we may consider the ratio $L_{\text{bol}}/L_{1.3}$. The millimetre luminosity $L_{1.3}$ is given by $L_{1.3} = 4\pi d^2 F_{1.3} \Delta\nu$, where d is the distance to the source, $F_{1.3}$ is the observed flux density and the bandpass is $\Delta\nu = 50\text{GHz}$. We estimate $L_{\text{bol}}/(10^3 \times L_{1.3}) = 20$ for FIRS 2, i.e. of the same order as Class 0 source values (André et al. 1993).

The total (gas + dust) circumstellar mass in the JCMT beam can be estimated using

$$M = \frac{S_{\nu} D^2}{B_{\nu,T} \kappa_{\nu}}$$

where symbols take their usual meanings and $\kappa_{\nu} \propto \nu^{\beta}$ (Hildebrand 1983). The estimated value (taking as reference $\lambda = 1.3\text{mm}$) of the mass is $M \approx 1.3 \cdot 10^{34} g$ or $\approx 6 M_{\odot}$. Assuming that this mass is distributed in a sphere equal in size to the $19''$ JCMT beam, then mass and particle densities are $\approx 1.0 \cdot 10^{-18} g\text{cm}^{-3}$ and $n \approx 5 \cdot 10^5 \text{cm}^{-3}$. These are lower limits since the mass is most likely distributed in a disk as suggested by the CO outflow associated with FIRS 2. The estimated $N(\text{H}_2)$ column density is $8.2 \cdot 10^{22} \text{cm}^{-2}$ and $A_V \approx 45$ mag (considering $A_V = 5.34 \cdot 10^{-22} N(\text{H}_2)$ mag). Again, these are

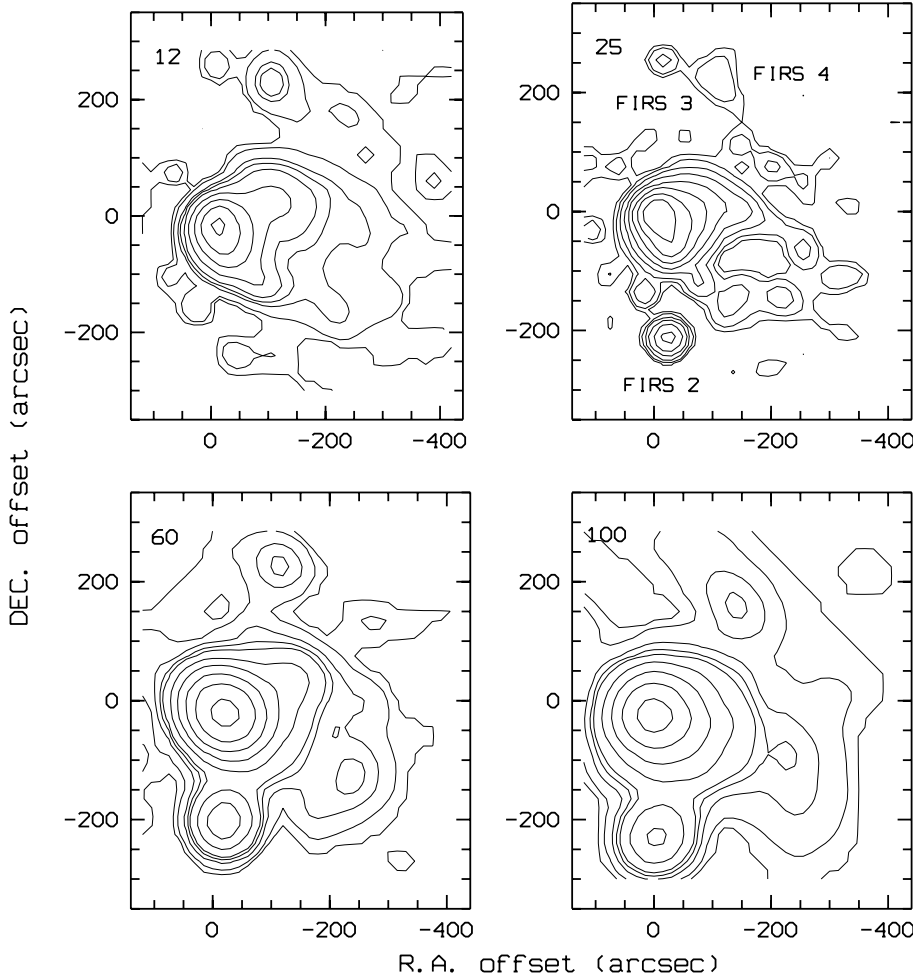


Fig. 1. HIRAS images of NGC 7129. Wavelength of each contour map is indicated. Point (0,0) corresponds to the 25 μm peak ($\alpha = 21^{\text{h}} 41^{\text{m}} 54.8^{\text{s}}$; $\delta = 65^{\circ} 53' 30''$). Far-infrared sources are indicated in the 25 μm map. Top-left: 12 μm image. Contours are 2, 3.5, 7, 9.5, 14, 28, 56, 112 and 224 MJy/sr. Top-right: 25 μm image. Contours are 3.2, 6.4, 12.5, 25, 50, 100, 200 and 400 MJy/sr. Bottom-left: 60 μm image. Contours are 12, 24, 48, 72, 96, 200, 400, 800, 1600 and 3200 MJy/sr. Bottom-right: 100 μm image. Contours are 30, 60, 120, 180, 240, 480, 960, 2000 and 4000 MJy/sr

Table 2. 25 μm positions and fluxes in Jy of FIRS 3 and FIRS 4 in NGC 7129

Source	α (1950.0)	δ (1950.0)	F(12 μm)	F(25 μm)	F(60 μm)
FIRS 3	$21^{\text{h}} 41^{\text{m}} 52.5^{\text{s}}$	$65^{\circ} 57' 45''$	0.3	0.8	
FIRS 4	$21^{\text{h}} 41^{\text{m}} 35.3^{\text{s}}$	$65^{\circ} 57' 02''$	1.3	1.3	9.4

lower limits. The estimated figures indicate that FIRS 2 is a very young stellar object. Note that a star with the luminosity of FIRS 2 is expected to be $M \sim 5M_{\odot}$. Since the mass of the dust and gas is of the same order of magnitude, we see that still a large fraction of the mass is in a dusty envelope or, most likely, in a circumstellar disk.

It is interesting to note that FIRS 2 shares its observational properties with those of the very young, low-mass Class 0 protostellar objects: 1. its SED is a single-temperature cool greybody; 2. most of the object mass is still in a circumstellar disk or envelope; 3. the $L_{\text{bol}}/L_{1.3}$ ratio is among the highest found for Class 0 sources, but much lower than the same ratio for the more evolved Class I sources. Class 0 objects are normally undetected in the 12 μm IRAS band, although some of them are - e.g. L 1448/mm (Bachiller et al. 1991) -; therefore, even if the weak 12 μm source discussed in the previous section was really associated with FIRS 2, the similarity between FIRS 2 and

Class 0 objects would remain. As pointed out before, the bolometric and submillimetre luminosities are indirect indicators of the stellar and circumstellar masses, respectively. Our estimates for FIRS 2 give a ratio $M_{\text{env}}/M_{*} \geq 1$ and the formal boundary for Class 0 and Class I sources is set at $M_{\text{env}}/M_{*} = 1$ (André 1997). A further characteristics of Class 0 objects is their association with highly collimated outflows with dynamical time scales $\leq 10^4$ years. In the case of FIRS 2, Edwards & Snell (1983) estimate a dynamical time for its associated outflow of 10^5 years. However, this estimate is based on the apparent size of the blue outflow, which has a secondary maximum at the position of the Herbig-Haro complex GGD 32/HH 103 field. Optical spectroscopy indicates that this complex of shocked gas is more likely associated with the expansion of the NGC 7129 cavity (Miranda & Eiroa, in preparation); consequently, the size of the FIRS 2 CO outflow and its dynamical time would be considerably smaller. If we estimate the dynamical time using the size of

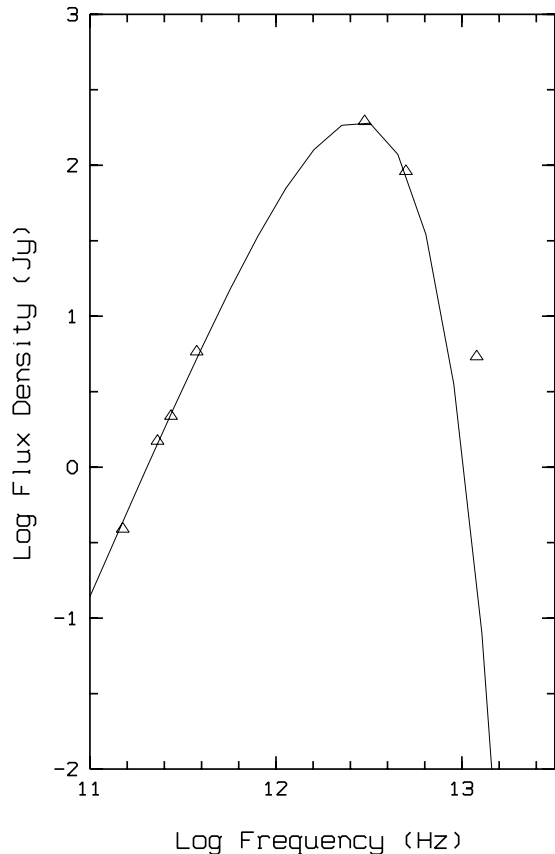


Fig. 2. SED of NGC 7129 FIRS 2. The solid line is a grey body consistent with the data (best χ^2 -fit) and has values $T = 35 K$, $\beta = 0.9$.

the red lobe, the result is $\approx 5 \cdot 10^4$ years, which is a value close to those of some Class 0 outflows, e.g. B 335 (Saraceno et al. 1996).

Considering the total luminosity, this parameter is much higher for our source than for any of the known Class 0 objects (see Bachiller 1996). Only, IRAS20050 - a Class 0 object which needs confirmation - has a luminosity of around 60% the luminosity of FIRS 2. This probably reflects the fact that FIRS 2 is a more massive protostellar object.

Concerning the dust characteristics around Class 0 objects, most of them have emissivity index values $\beta \approx 1.5 - 2$, similar to the interstellar medium value; e.g. André et al. (1993) and Ward Thompson et al. (1995b) estimate $\beta = 1.5$ for the prototypical Class 0 objects VLA 1623 and NGC 2264G respectively, although smaller values have also been estimated, e.g. HH 24mms with β in the range 0.8 - 1.5 (Ward Thompson et al. 1995a). In the case of FIRS 2, $\beta \approx 1.5$ provides a very unsatisfactory fit. Dust particles in circumstellar disks around T Tauri stars have values $\beta \leq 1$ (Beckwith & Sargent 1991), i.e. similar to the value found by us for FIRS 2. This small β value has been interpreted as due to grain growth and fractal formation. In this scenario, the grains around FIRS 2, $\beta = 0.9$, would be larger than the interstellar solid particles. An alternative, however, has recently been proposed by Chandler et al. (1995). These authors found a β value of 0.68 in the disk around

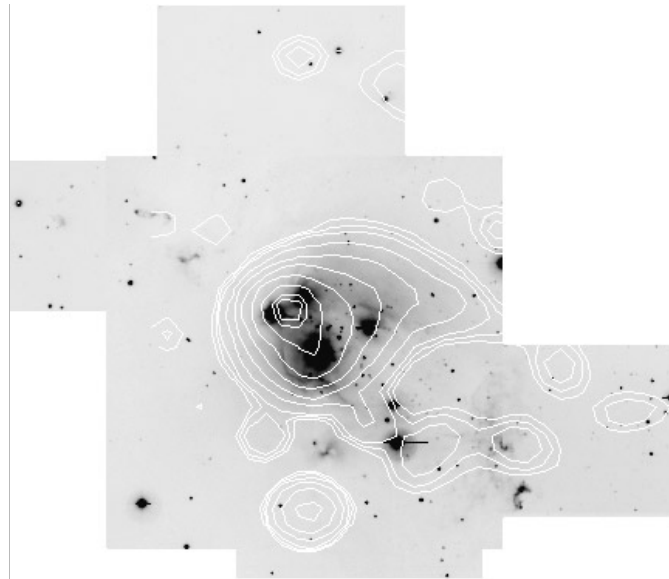


Fig. 3. IRAS $25\mu\text{m}$ image overlaid on a gray-scale [SII] image of NGC 7129

HH 24mms and suggested that such low β values may be a feature of a high density environment as may also be the case in our source. Summarizing, FIRS 2 is a high luminosity young stellar object which shares the typical properties of the very young, low-mass Class 0 objects and is therefore the highest mass counterpart of these extremely young sources.

3.2. The far-infrared emission in NGC 7129

Several interesting morphological features are revealed by the IRAS maps (Fig. 1). At 12 and $25 \mu\text{m}$, the emission is clearly dominated by FIRS 1 surrounded by a diffuse extended emission mainly directed towards the southwest; a very strong gradient of the emission towards the E-NE of FIRS 1 is observed, meanwhile towards the W-SW the emission is smoother. At 60 and $100 \mu\text{m}$, the diffuse emission extends to a larger area, although FIRS 1, FIRS 2 and also the strong gradient E-NE of FIRS 1 are also very prominent at these wavelengths. FIRS 1 coincides with the HAeBe star LkH α 234; however, a significant contribution can come from the recently discovered mid-infrared companion IRS 6, particularly at the longest wavelengths (Weintraub et al. 1994, Cabrit et al. 1997).

At 12 and $25 \mu\text{m}$ the extended emission has a conical shape with FIRS 1 at its apex and two protusions surrounding a cavity. The cavity is also remarkable in the static CO (J=1-0) emission gas (Bertout 1987) and in the optical. Fig 3. shows the $25 \mu\text{m}$ IRAS image superimposed on a [SII] mosaicing-image of the region, taken at the Calar Alto 3.5 m telescope. The optical nebulosity has a very sharp edge towards the NE of LkH α 234, as does the far-IR emission, although the later extends farther towards the NW; both wavelengths reveal the cavity and arms and filaments surrounding it. Even the strongest contours at 12 and $25 \mu\text{m}$, i.e. those delineating the FIRS 1 peak, are morphologically similar to the optical appearance of LkH α 234 and

its immediate surroundings as well as to the near-IR cometary nebulosity detected at this position, which is most likely associated with the infrared companion (Weintraub et al. 1996). All these facts are consistent with the idea that there is a good coupling between the gas and dust in the region and that the dust responsible for the 12 and 25 μm emissions is the same dust that produces the NGC 7129 reflection nebulosity even in the closest surroundings of the LkH α 234 field. At the western end, the cavity is closed by diffuse, shocked optical emission in which many HH condensations are embedded, among them GGD 32 and HH 103 (Eiroa et al. 1992, Miranda & Eiroa, in preparation). It is interesting to point out that the 25 μm emission also ends at this position approximately.

The total integrated IRAS luminosity of the region is $3.1 \cdot 10^3 L_{\odot}$, and an extrapolation to infinite wavelengths gives $4.5 \cdot 10^3 L_{\odot}$. This estimate makes reasonable the assumption that the dust in NGC 7129 is heated by LkH α 234 and its companion, FIRS 2 and also by other young B stars in the field, as has been previously suggested (e.g. Harvey et al. 1984). Values of the dust colour temperatures and the 100 μm optical depth estimated from the IRAS data are similar to those found by Harvey et al. (1984) and Bechis et al (1978) and so are not included here.

Two alternatives have been proposed to explain the observed cavity in NGC 7129. Bertout (1987) attributes the cavity to the stellar wind from LkH α 234 which would have excavated the molecular cloud. Ray et al. (1990) point out that the cometary-like appearance of the NGC 7129 reflection nebula and the optical jet along the cavity axis support this idea. The recent discovery of a mid-IR companion of LkH α 234, which could be the driving source of the optical jet, does not contradict this scenario. On the other hand, Bechis et al. (1978) and Mitchell & Matthews (1994) favour the idea that the cavity has been produced by older stars in the region, i.e. BD +65° 1637 and BD +65° 1638; in this case, the argument is that LkH α 234 is embedded in a CO molecular ridge sharply bounded to the west by the cavity, suggesting a shell formation event and triggered star formation. In our opinion, the IRAS data do not rule out any of the alternatives, although a sharp gradient towards the west is not observed in the dust emission as it is in the CO static gas. Optical spectroscopic data and proper motions in the GGD 32/HH 103 field are also compatible with both alternatives (Miranda & Eiroa, in preparation).

4. Conclusions

The major finding revealed by the data presented in this work is that NGC 7129 FIRS 2 can be considered as an intermediate-mass counterpart of the low-mass Class 0 objects; in other words, we could describe FIRS 2 as an intermediate-mass submillimetre protostar. The source is probably the youngest object of its kind known at present, and will probably evolve into an HAeBe star. We consider it is of high interest to find more similar objects, so that a low-mass/intermediate-mass submillimetre protostar sample could be studied as is done with the more evolved T Tauri/HAeBe stars.

Acknowledgements. The JCMT is operated jointly by the UK Particle Physics and Astronomy Research Council, the Netherlands Organization for the Advancement of Pure Research, the Canadian National Research Council, and the University of Hawaii. C.E. is very grateful to Dr. P. Weselius for his kind hospitality at SRON, Groningen, during a stay in summer 1995 when the IRAS data were reduced. C.E. and J. Palacios are supported in part by Spanish Grant DGICYT PB94-0165.

References

- André P. 1997, in “Herbig-Haro flows and the birth of low mass stars”, B. Reipurth and C. Bertout, eds., KLUWER, p. 483
- André P., Ward-Thompson D., Barsony M. 1993, ApJ 406, 122
- Bachiller R. 1996, ARA&A 34, 111
- Bachiller R., André P., Cabrit C. 1991, A&A 241, L43
- Bechis K.P., Harvey P.M., Murray F.C., Hoffman W.F. 1978, ApJ 226, 439
- Beckwith S.V.W., Sargent A.I. 1991, ApJ 381, 250
- Bertout C. 1987, in “Circumstellar Matter” I. Appenzeller and C. Jordan, eds., REIDEL, p. 23
- Bontekoe T.J.R., Koper E., Kester D.J.M. 1994, A&A 284, 1037
- Cabrit S., Lagage P.-O., McCaughrean M.J., Olofsson G. 1997, A&A 321, 523
- Casali M.M., Eiroa C., Duncan W.D. 1993, A&A 275, 195
- Chandler C.J., Koerner D.W., Sargent A.I., Wood D.O.S. 1995, ApJ 449, L139
- Davis C.J., Dent W.R.F., Matthews H.E., Aspin C., Lightfoot, J.F. 1994, MNRAS 266, 933
- Duncan W.D., Robson E.I., Ade P.A.R., Griffin M.J., Sandell, G. 1990, MNRAS 243, 126
- Edwards S., Snell R.L. 1983, ApJ 270, 605
- Eiroa C., Gómez de Castro A.I., Miranda L.F. 1992, A&AS 92, 721
- Eiroa C., Miranda L.F., Anglada G., Estalella R., Torrelles J.M. 1994, A&A 283, 973
- Griffin M.J., Ade P.A.R., Orton G.S., et al. 1986, Icarus 65, 244
- Güsten R., Marcaide J.M. 1986, A&A 164, 342
- Hartigan P., Lada C.J. 1985, ApJS 59, 383
- Harvey P.M., Wilking B.A., Joy M. 1984, ApJ 278, 156
- Hildebrand R.H. 1983, QJRAS 24, 267
- Magakian T.Yu. 1983, Soviet Astron. Lett 9, 83
- Magakian T.Yu., Movsesian T.A., 1997, Astron. Reports 41, 483
- Miranda L.F., Eiroa C., Fernández M., Gómez de Castro A.I. 1994, A&A 281, 864
- Miranda L.F., Eiroa C., Gómez de Castro A.I. 1993, A&A 271, 564
- Mitchell G.F., Matthews H.E. 1994, ApJ 423, L55
- Orton G.S., Griffin M.J., Ade P.A.R., 1986, Icarus 67, 289
- Palla F., Stahler S.W. 1990, ApJ 360, L47
- Palla F., Stahler S.W. 1993, ApJ 418, 414
- Racine R. 1968, AJ 73, 233
- Ray T.P., Poetzel R., Solf J., Mundt R.: 1990, ApJ 357, L45
- Rodríguez L.F., Moran J.M., Ho P.T.P., Gottlieb E.W. 1980, ApJ 235, 845
- Saraceno P., André P., Griffin M., Molinari S. 1996, A&A 309, 827
- Shevchenko V.S., Yakubov S.D. 1989, Sov. Astron. 33, 370
- Strom S.E., Vrba F.J., Strom K.M. 1976, AJ 81, 638
- Ward-Thompson D., Chini R., Krügel E., André P., Bontemps S. 1995a, MNRAS 274, 1219
- Ward-Thompson D., Eiroa C., Casali M.M. 1995b, MNRAS 273, L25
- Weintraub D.A., Kastner J.J., Mahesh, A. 1994, ApJ 420, L87
- Weintraub D.A., Kastner J.H., Gately I., Merrill K.M. 1996, ApJ 468, L45